ANL-7626

Argonne National Laboratory

HYBRID SIMULATIONS OF ENERGY- AND SPACE-DEPENDENT CORE DYNAMICS

by

J. C. Carter, N. F. Morehouse,
L. W. Amiot, and F. J. Maletich

The facilities of Argonne National Laboratory are owned by the United States Government. Under the terms of a contract (W-31-109-Eng-38) between the U. S. Atomic Energy Commission, Argonne Universities Association and The University of Chicago, the University employs the staff and operates the Laboratory in accordance with policies and programs formulated, approved and reviewed by the Association.

Printed in the United States of America
Available from
Clearinghouse for Federal Scientific and Technical Information
National Bureau of Standards, U. S. Department of Commerce
Springfield, Virginia 22151
Price: Printed Copy $3.00; Microfiche $0.65

ANL-7626
Mathematics and Computers

ARGONNE NATIONAL LABORATORY
9700 South Cass Avenue
Argonne, Illinois 60439

HYBRID SIMULATIONS OF ENERGY- AND SPACE-DEPENDENT CORE DYNAMICS

by

J. C. Carter
Reactor Analysis and Safety Division

N. F. Morehouse, L. W. Amiot,
and F. J. Maletich
Applied Mathematics Division

February 1970

TABLE OF CONTENTS

LIST OF FIGURES

HYBRID SIMULATIONS OF ENERGY- AND SPACE-DEPENDENT CORE DYNAMICS

by

J. C. Carter, N. F. Morehouse,
L. W. Amiot, and F. J. Maletich

ABSTRACT

A small and relatively slow hybrid computer has been assembled for the purpose of gaining experience and evaluating the potential of simulating large mathematical models of reactor systems.

The first simulation presented is a model consisting of the two-group, space- and time-dependent neutron-diffusion equations with delayed groups, two-dimensional heat transfer in each of three core regions, and reactivity feedbacks from each region due to Doppler effect and changes in the physical properties of fuel and coolant. The cylindrical volume of a 1000-MWe fast reactor is divided into five radial increments and six axial increments. Coupling between radial and axial increments is by heat flow and neutron diffusion.

The solution over the volume of the core is achieved by multiplexing equations and by using iterative techniques. The equations are written to define average values of variables within the volume of each increment of the cylindrical core. At each axial increment, the reactivity feedback resulting from a forced variation of an energy-, space-, and time-dependent variable, such as the fission cross section in a given geometric increment, is calculated and stored in the computer memory. The exit values of the variables from the first axial increment become the initial value to the second axial increment, and so on until the volume of the core is covered. The calculation is repeated until convergence is achieved.

The responses of the model to perturbations of time-dependent variables in a given energy group or space mode are presented and analyzed. These perturbations are in the form of impulses, steps, ramps, and oscillations in the neutron production or in any other variable in the equations comprising the model of the reactor system.

I. INTRODUCTION

The dynamic system of a 1000-MW fast reactor is simulated on a hybrid computer. This system consists of three categories of physical phenomena--neutronic, thermodynamic, and mechanical. The source of power is in the neutronic category, the sink is in the thermodynamic category, and the restraints are imposed by the mechanical category of phenomena.

After a disturbance in the system, the neutrons redistribute in energy, space, and time. The system may regain equilibrium if the feedbacks from the thermodynamic and mechanical to neutronic phenomena have been designed to dampen the perturbations. Equilibrium exists in all categories of the phenomena occurring in the reactor when the effective reactivity for the system is equal to 1.

There is a very complex interaction of neutronic, thermodynamic, and mechanical phenomena within a reactor core. The mathematical model presented here of the dynamic system, in which these phenomena interact, is currently very much oversimplified.

The purpose of presenting this simple mathematical model of a 1000-MW fast reactor is to indicate the potentialities of the hybrid computer for simulating a very large dynamic system in which there are phenomena with widely varying frequency responses and intricate coupling.

The emphasis in this first effort is on developing techniques for (1) handling a small number of energy and volume increments and (2) linking equations with widely varying frequency characteristics. The relationships between physical changes in the core and the neutronic variables and the coupling between energy groups and geometric regions are the aspects that are oversimplified now. As the limitations on the computer facilities are extended, the physical changes and coupling can be better represented and there can be more energy groups and smaller increments of core volume.

Since the response of the neutronic phenomenon is very much faster than the responses of the thermodynamic and mechanical phenomena, all time-dependent neutronic equations are simulated on the analog component of the hybrid, and all thermodynamic and mechanical equations are programmed to be multiplexed on the digital component.

It is very expensive to simulate a realistic mathematical model of a reactor core, since the amount of computing hardware and programming effort rises rapidly when the model consists of more than the point kinetics and a one-region core.

Theoretically, there is no limitation to increasing the number of energy groups, the space increments, and the addition of reactor auxiliaries to the system, except the economic one. When more than one energy group, more than one core region, and the principal feedbacks are included in the model, it is necessary to consider the type of computer on which the model can be most effectively simulated. The types of computers currently available are the digital, the analog, and the hybrid.

The simulation of large dynamic systems appears to have two trends: One is toward larger digital computers, and the other is toward hybrid computers. The hybrid is a combination of analog and digital, wherein numerical analysis, a knowledge of computers, and programming skill are substituted for computing hardware.

A brief description of each type of available computer is followed by a description of the mathematical model of a 1000-MW reactor, the techniques of performing the simulation, the result of perturbing the model, a general discussion, and the computing program.

II. TYPES OF COMPUTERS

A. Digital

The modern digital computer, developed after 1950, has the ability to perform arithmetic operations at very high speeds together with a large, fast storage capability for storing data and instructions. It thus became possible to integrate many systems of differential equations by replacing the infinitesimal operators of integration and differentiation by arithmetic operators of sufficient accuracy to permit an accurate solution. In theory, if a digital computer has sufficient speed and computes with numbers that have enough digits, almost any system of differential equations can be solved. However, the machines in existence today do not have anywhere near the capacity to solve some systems of differential equations occurring in space exploration and proposed reactor simulations. The computer limitations may in many cases be overcome by ingenious programming.

Theoretically, any model can be put on the digital computer, but with a large amount of programming effort and with the technique of overlaying. Lack of mathematical rigor in transforming equations and incompatibility in time incrementation of the equations of the respective categories often result in truncation errors and instability when the modular codes to solve these equations are in series and parallel.

B. Analog

An analog computer is one that uses electronic components for the direct simulation of integration, differentiation, and the arithmetic operations of addition, subtraction, multiplication, and division. Before about 1950, it was the only type of computer capable of solving large dynamic systems of differential equations.

The large number of computer components necessary for simulating even the point-kinetics one-region model of a reactor rules out the pure analog computer for any larger mathematical models.

C. Hybrid

A hybrid computer is a combination of the two types of computer (analog and digital) into a single integrated computing system. Hybrid computers are new and have potentialities for the simulation of large dynamic systems of coupled categories of phenomena with widely varying frequency characteristics.

Since not all systems of differential equations can be solved on digital computers, and since analog and digital computers employ very different methods of solving the systems of equations, it is not surprising that there are equations of interest that can be solved on an analog computer, but cannot be solved satisfactorily on a digital computer. Therefore, there came into existence a computer known as a hybrid computer, which combines an analog and a digital computer into one large integrated computing system. At present two or three hybrid computers are being sold, but they are still in their infancy and most of the basic software and computing technique still remains to be developed. Although solid-state electronics enable the analog-computer part of a hybrid computer to be entirely controlled from the digital computer (including patching connections, setting potentiometers, and checking out the problem), the present hybrid computers fall considerably short of their potential. All the hybrid computers presently on the market require manual patching, and many require manual checkout and manually set potentiometers. Consequently, instead of controlling the entire computer from one digital computer, as would be possible in a "state-of-the-art system," presently marketed hybrid computers require the programmer to get involved with the computer hardware. This is currently the biggest drawback of commercially available hybrids.

Eventually the analog component will be entirely controllable from the digital components and the mechanics of programming for the hybrid will be the same as programming for an all-digital computer.

D. Argonne's Hybrid

Argonne's hybrid consists of the existing analog computer and an IBM 1130 digital computer, which communicate by means of an interface designed and built at Argonne.

The analog computer consists of two Electronic Associates 131-R consoles and two Reeves 550 consoles. The entire system has about 300 amplifiers, although much of the equipment is out of date.

The IBM 1130 is equipped with a disk bulk storage, a card-reader punch, and a line printer. The entire computer is either FORTRAN or assembly language programmable at the programmer's option.

Although this computer is far from representing the state of the art, particularly in terms of convenience for the programmer and operator, it does permit a number of hybrid applications to be developed and tested.

The amount of investigating that has been done indicates that many reactor simulations can be done effectively on a computer composed of both analog and digital components, wherein each component is used for the type of equations for which it is best suited.

III. THE EQUATIONS COMPRISING THE MODEL

The mathematical model of the system consists of the two-group, space- and time-dependent, neutron-diffusion equations with delayed neutrons; two-dimensional heat-transfer equations in each of three core regions; and a reactivity-feedback equation relating Doppler effect and temperature variations in the core materials of each core region to the variables in the neutron-diffusion equations.

The equations that define the phenomena of the respective categories have widely varying frequency responses and complex interactions between those variables that are common to each category. Thus, the attainment of continuity and compatability in energy, space, and time is difficult to achieve in a simultaneous solution of all the equations comprising the mathematical model of the reactor system.

The differencing schemes for the equations comprising the models, particularly with respect to time, present a formidable task in numerical analysis and programming in order to couple the equations in one category to those in another. This can be made easier when the hybrid computer is used, because the equations with high-frequency response are solved on the analog components.

In every simulation of a model of a dynamic system, the characteristics of each equation must be analyzed and decisions reached as to which equations of the model will be programmed for the digital components and which equations for the analog components.

The physical arrangement of the reactor core is that of an assembly of spaced UO_2 rods in the form of a right cylinder through which sodium flows longitudinally. The core is surrounded by a neutron reflector. The radial and axial regions into which this reactor is divided are shown in Fig. 1. The numerical values of the physical phenomena within these cylindrical increments are the average for the increment.

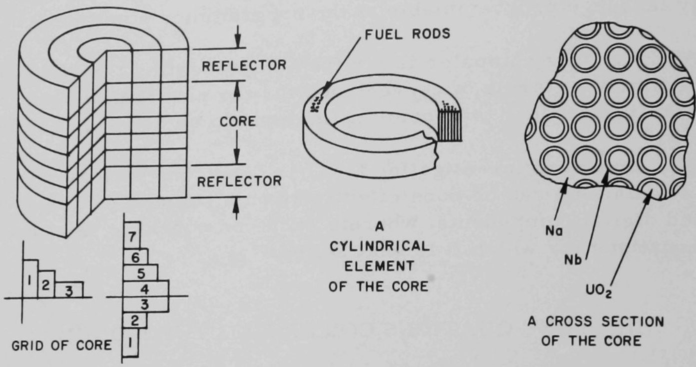

Fig. 1. The Radial and Axial Incrementation of the Core

Figure 2 shows a schematic representation of the basic model. The energy groups and radial regions are coupled by neutron flux. The axial regions are coupled by the continuity of the sodium flowing axially along the fuel rods.

The equations comprising the model are presented here and treated in detail in Appendix B. They are considered in three categories: the neutronic, the thermodynamic, and the feedback equations.

A. Neutronic Equations

The two-group neutron-diffusion equations are expressed in the form

$$\frac{1}{v_{1i}} \times \frac{\partial \phi_{1i}}{\partial t} = D_{1i}\nabla^2\phi_{1i} - \Sigma_{1ia}\phi_{1i} - \Sigma_{1is}\phi_{1i} + (1-\beta)[X_1\nu_{2i}\Sigma_{2if}\phi_{2i}$$

$$+ X_1\nu_{2i}\Sigma_{1if}\phi_{1i}] + \sum_{k=1}^{6}\lambda_{ki}C_{ki}, \tag{1}$$

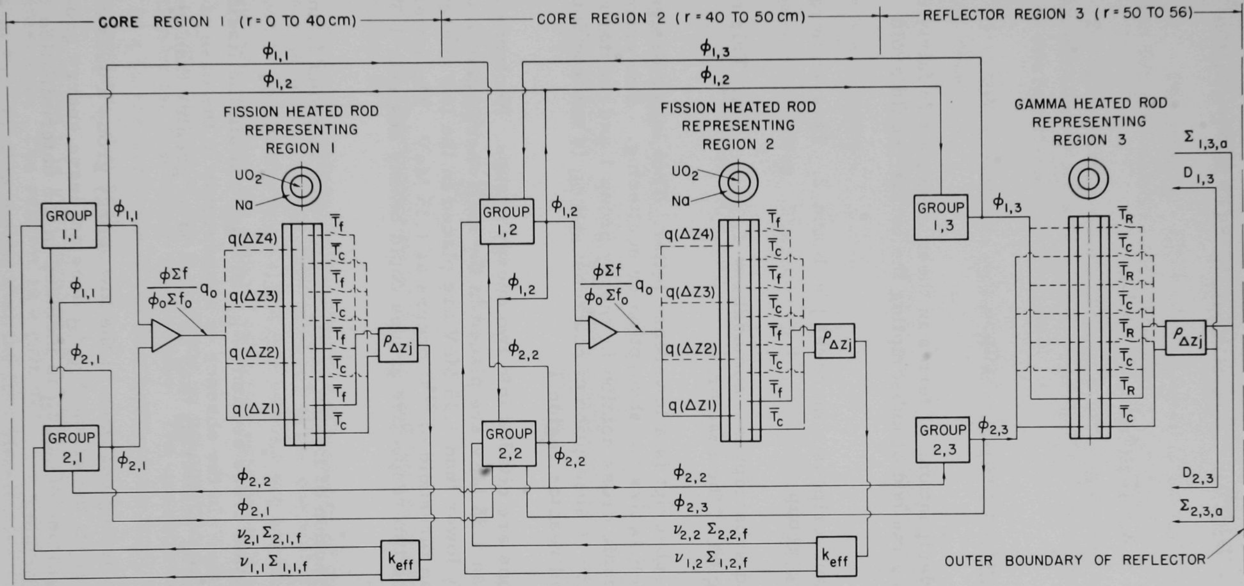

Fig. 2. Schematic Diagram of the Mathematical Model of the Reactor. ANL Neg. No. 113-2635 Rev. 1.

$$\frac{1}{v_{2i}} \times \frac{\partial \phi_{2i}}{\partial t} = D_{2i}\nabla^2\phi_{2i} - \Sigma_{2ia}\phi_{2i} + \Sigma_{1is}\phi_{1i} + (1-\beta)[X_2\nu_{1i}\Sigma_{1if}\phi_{1i}$$

$$+ X_2\nu_{2i}\Sigma_{2if}\phi_{2i}] + \sum_{k=1}^{6} \lambda_{ki}C_{ki}, \tag{2}$$

and

$$\frac{\partial C_k}{\partial t} = \beta\Sigma_{1if}\phi_{1i} + \beta\Sigma_{2if}\phi_{2i} - \lambda_k C_k. \tag{3}$$

Since the designations of terms in these equations is fairly complicated, the following method of subscripting the terms should avoid confusion:

The first subscript is a numeral $j = 1$ and 2. This numeral is that of the eneryg group.

The second subscript is a numeral $i = 1, 2, 3, ..., n$. This numeral designates the region of the reactor.

The third subscript is a lowercase letter. This letter designates the phenomena such as fission, absorption or scattering. For example, Σ_{14a} is a macroscopic cross section in energy group 1 and reactor region 4, and the phenomenon is absorption of neutrons; and ϕ_{21} is neutron flux in energy group 2 and reactor region 1.

The neutrons are divided into two energy groups. Neutrons of energy greater than 1.35 MeV are placed in the high energy group, and neutrons of energy lower than 1.35 MeV are placed in the low energy group. The fission threshold of ^{238}U occurs at 1.35 MeV. The lower and upper bounds of the two respective groups could be any desired; 1.35 MeV is just convenient.

X_1 is the fraction of fission neutrons produced in group 1, and X_2 the fraction in group 2.

The absorption cross sections Σ_{1ia} and Σ_{2ia} contain the fission and capture cross section. In the absence of a moderator in the case of a fast reactor, inelastic scattering may be equal to or greater than elastic scattering.

Since a scattering collision in the low energy group 2 does not remove neutrons from the group, $\Sigma_{2is}\phi_{2i}$ does not leave energy group 2. However, the magnitude of $\Sigma_{2is}\phi_{2i}$ is included in the determination of the diffusion coefficients.

The following assumptions are made:

1. The reactor will be divided into a number of regions with provision for a solution in each region.

2. The energy-dependence will be taken into account by dividing the energy spectrum into n groups and solving an equation for each energy group in each region.

3. $\nabla D \nabla \phi$ must be approximated as a function of one space variable only.

For a unit volume in a homogeneous region,

$$\frac{\partial \phi}{\partial t} = \nabla D \nabla \phi - \Sigma_a \phi + S, \tag{4}$$

for one energy group. Since $\phi = nv$ and D are constant in each region,

$$\frac{1}{v}\frac{\partial \phi}{\partial t} = D\nabla^2 \phi - \Sigma_a \phi + S. \tag{5}$$

For an arbitrary volume V,

$$\iiint \frac{1}{v}\frac{\partial \phi}{\partial t}\, dV = \iiint D\nabla^2 \phi \, dV + \iiint (S - \Sigma_a \phi)\, dV. \tag{6}$$

But

$$\iiint \nabla^2 \phi \, dV = \iint D\nabla_i \phi \, dS, \tag{7}$$

where $\nabla_i \phi$ is the component of $\nabla \phi$ directed toward the outward normal to the surface S.

Since the volume integral of the divergence of the neutron current can be replaced by the surface integral of the current (i.e.,$\nabla_n \phi$), difficulties inherent in approximating second derivatives are avoided. This manipulation will also reduce the amount of analog equipment needed.

The solution of Eq. 6 involves an assumption as to the spatial variation of the flux within each region. The assumption used here is that there is a linear variation in the flux between the midpoint of a region and and boundary of that region.

Equation 6 is still three-dimensional, but it may be reduced to one dimension. The reactor is a cylinder with three annular regions (as shown in Fig. 1); this means that the flux distribution will be a function of the radius and the height. If a cosine variation is assumed in the axial direction, a correction for axial leakage can be added to the absorption loss in each region. Therefore, $D\nabla_n\phi$ can be calculated with respect to one space variable. The calculation $DV_n\phi$ can be done with respect to one space variable if the axial buckling is assumed.

It is now possible to determine the function that will describe the diffusion between two regions. The subscripts here refer to regions.

Two assumptions are made:

1. Within a region, a linear variation in flux exists from the center to the boundary (see Fig. 3).

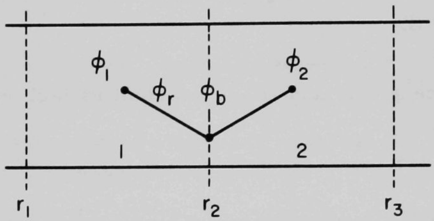

Fig. 3
Regional Neutron Flux Coupling

2. At an interface,

a. $\lim_{\epsilon \to 0} \phi(r + \epsilon) = \lim_{\epsilon \to 0} \quad (r - \epsilon);$

b. $\lim_{\epsilon \to 0} D_1 \nabla \phi(r + \epsilon) = \lim_{\epsilon \to 0} D_2 \nabla \phi(r - \epsilon).$

In the right semiregion of 1,

$$\nabla\phi(r) = \frac{2(\phi_b - \phi_1)}{r_2 - r_1} \tag{8}$$

In the left semiregion of 2,

$$\nabla\phi(r) = \frac{2(\phi_2 - \phi_b)}{r_3 - r_2} \tag{9}$$

According to assumption 2b and Eqs. 1 and 2,

$$2D_1 \frac{(\phi_b - \phi_1)}{r_2 - r_1} = 2D_2 \frac{(\phi_2 - \phi_b)}{r_3 - r_2}, \tag{10}$$

and

$$\phi_b = \frac{\frac{D_2}{r_3 - r_2}\phi_2 + \frac{D_1}{r_2 - r_1}\phi_1}{\frac{D_1}{r_2 - r_1} + \frac{D_2}{r_3 - r_2}} \tag{11}$$

Let

$$D_i' = \frac{D_i}{r_{i+1} - r_i}. \tag{12}$$

Then

$$\phi_b = \frac{D_2'\phi_2 + D_1'\phi_1}{D_1' + D_2'}. \tag{13}$$

It is now possible to express $D_1 \nabla\phi$ as a function of ϕ_1 and ϕ_2 by use of Eqs. 8 and 13, as follows:

$$D_1\nabla\phi = \frac{2D_1'\phi_2 + D_1'\phi_1}{D' + D_2'} - \phi_1 = \frac{2D_1'D_2'}{D_1 + D_2}(\phi_2 - \phi_1). \tag{14}$$

Equation 14 is valid in any interior region for half the region.

The total diffusion L across the interregional boundaries for an interior region is

$$L = \iint D\nabla_i \phi \, dS \, \frac{2D_{i-1}'D_i'}{D_{i-1}' + D_i'}(\phi_i - \phi_{i-1}) S_i$$

$$+ \frac{2D_i'D_{i+1}'}{D_i' + D_{i+1}'}(\phi_i - \phi_{i+1}) S_{i+1}, \tag{15}$$

where S_i is the total surface bounding the left side of region n, and S_{i+1} is the total surface bounding the right side of region i. At an outer boundary, the inward neutron current is 0. Thus,

$$J = \frac{6\phi}{4} + \frac{\lambda t}{6}\frac{d\phi}{dr} = 0. \tag{16}$$

The following substitutions can be made in Eq. 9:

$$3D = \lambda_t, \tag{17}$$

and

$$\frac{d\phi}{dr} \simeq - \frac{\phi_n - \phi_b}{(r_{i+1} - r_i)/2}. \tag{18}$$

The neutron current out of the reactor is

$$J = \frac{\phi_b}{4} - \frac{\lambda t}{6} \frac{d\phi_b}{dr}. \tag{19}$$

The total leakage out of the reactor is

$$L \cong J + S_4 = J\phi_3 S_4.$$

In accordance with the above reasoning and assumptions, the two-group time-dependent diffusion equations are transformed into a set that can be simulated on an analog computer. The set of equations for each of the three regions of the core are presented in Appendix B.

B. Thermodynamic Equations

The thermodynamic equations consist of the heat-transfer equations for the fuel elements and for the coolant. Both the analog and digital programs for these equations are presented.

1. Heat-transfer Equations Pertaining to a Fuel Element

The heat-transfer equations are written for a cylindrical fuel cell, shown in Fig. 4. The following are the assumptions:

a. The internal heat-generation rate is symmetric with respect to the longitudinal axis of the cell, and the materials are isotropic.

b. The axial conduction of heat and the radial variation of the coolant temperature are neglected.

c. Materials do not have phase changes (fuel melting and coolant boiling) during transience. Further, there is no large-scale disassembly of the core.

Under these assumptions, the heat-conduction equations are written in one-dimensional space--namely, r at positions z along the longitudinal axis:

$$c\rho r \frac{\partial T}{\partial t} = \frac{\partial}{\partial r}\left(Kr\frac{\partial T}{\partial r}\right) + rq(r,z,t) \qquad \text{(for fuel)}, \tag{20}$$

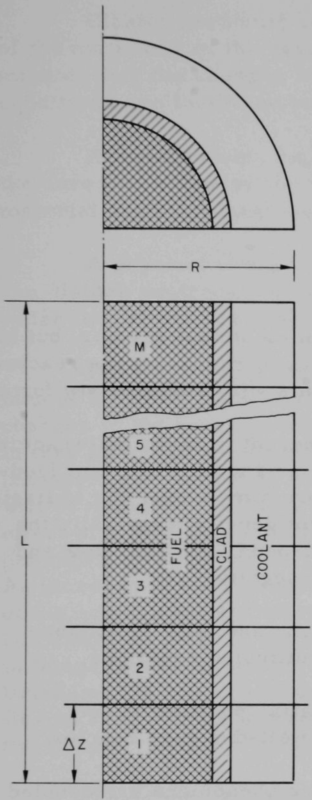

Fig. 4. Diagram of a Cylindrical Fuel Cell

and

$$c\rho r \frac{\partial T}{\partial t} = \frac{\partial}{\partial r}\left(Kr\frac{\partial T}{\partial t}\right) \qquad (21)$$

(for bond or cladding),

where

T = the temperature,

c = the specific heat,

ρ = the density,

K = the thermal conductivity,

and

q = the internal volumetric heat-generation rate.

The boundary conditions are:

$$\left.\frac{\partial T}{\partial r}\right|_{r=0} = 0 \text{ (assuming the material to be isotropic)}, \qquad (22)$$

and

$$-K\left.\frac{\partial T}{\partial r}\right|_{r=R} = h(T_R - T_c) \equiv Q, \qquad (23)$$

where T_R is the temperature at the surface of the cladding, and T_c is the average coolant temperature. The surface heat-transfer coefficient h is a function of temperature and coolant flowrate. Q represents the heat transferred per second per unit area of the boundary between the fuel cladding and the coolant.

The rise in coolant temperature for any axial increment may be obtained by writing the heat-balance equation. This equation, in its differential form, may be stated as

$$\frac{\partial}{\partial t}(\rho c T c) + \frac{\partial}{\partial z}(GcTc) = \Lambda Q, \qquad (24)$$

where

ρ = the density,

c = the specific heat

and

T_c = the temperature of the coolant.

C. Feedback Equations

There are a large number of feedbacks in the actual reactor, but in the system of nonlinear equations considered here to represent the reactor phenomena, only three are used, and these are in a very rudimentary form.

One is the Doppler feedback, which is inherent in large fast reactors. It is prompt and nearly always negative. The second most important feedback results from changes in fuel density and core dimensions due to fission heating. The third comes from changes in coolant density, especially the change associated with boiling. These last two depend upon heat flow and therefore have time lags. They also are usually negative.

All three feedbacks alter the cross sections and thus the balance between loss and production as described in the diffusion equations.

Neutrons change in energy levels and spatial position in an endeavor to maintain neutronic equilibrium in a well-designed reactor.

The neutronic, thermodynamic, and elastic phenomena are coupled and interact so the reactor cannot be in a steady state (k_{eff} = 1) unless all three are in equilibrium throughout the entire volume of the reactor. Since the neutronics, thermodynamics, and mechanics are not separate and independent in a reactor, the equations in the mathematical model describing the phenomena associated with them must satisfy the conditions for continuity and conservation of energy transformations.

Neutronic continuity is maintained in energy and in space in the multigroup diffusion equation. This continuity is maintained by virtue of the fission spectrum and the up and down scattering. In space, continuity is maintained by diffusion throughout the volume of the core.

Thermodynamic continuity is maintained by fluid flow and heat transfer.

Elastic continuity is accomplished by elastic and plastic deformation of the materials of the reactor. The core structure is statically indeterminate; thus the changes in dimensions following perturbation of steady-state conditions are those compatible with strain-energy equilibrium.

At equilibrium, the production of neutrons throughout the volume of the core just balances the loss of neutrons by absorption in nonfissionable material and by leakage out of the core.

A physical change within the core or an outside source of neutrons can disturb neutronic equilibrium with a consequent change in fission rate, which in turn disturbs thermodynamic and mechanical equilibrium.

Physical things that affect equilibrium are changes in the temperature of the core materials, changes in the density of core materials, changes in the phase of core materials, and mechanical changes. These in turn affect the cross sections for fission, absorption, scattering, and transport and constitute a feedback, which, if the core is properly designed, will be negative and cause the reactor to try to regain equilibrium. The effect of temperature on those isotopes that have resonances results in the principal feedback for fast reactors. It is known as the Doppler feedback. An increase in temperature and the resultant increase in thermal motion of the nucleus has the effect of broadening the resonance. Uranium-238 has a number of resonances. A large one occurs at 6.5 eV; thus an increase in temperature causes an increase absorption and a negative feedback. Uranium-235 has a resonance at 1.1 eV, which causes an increase in fission rate with an increase in temperature. The negative component of the Doppler feedback usually predominates.

The effect of increasing temperature on core materials and coolant is that of causing them to expand, thus decreasing macroscopic cross sections but increasing the dimensions and shape of the core. In some poorly designed reactors, the core tries to assume the shape of a hyperbola; this is known as the bowing effect.

If the temperature increases above the design level, the fuel may melt and the coolant boil. The diffusion coefficient varies inversely as the transport cross section, which is a function of neutron energy.

The cross sections, dimensional changes, and densities are not expressed as functions of energy and/or temperature in the neutron-diffusion equation. Instead, the following customary expression for reactivity feedback is used in this simulation:

$$\rho = a \,\ell n \left(1 + \frac{\Delta T_f}{T_0}\right) + b\Delta T_f + c\Delta T_c, \tag{25}$$

where ρ pertains to a volumetric increment of the core. When ρ for the entire volume is 0, the simulated system on the computer is in equilibrium.

If any cross section or diffusion coefficient is changed, the system is perturbed and the variation in neutron flux of any group at any point in the core can be seen as a function of time on an oscilloscope attached to the computer.

The relationship between the fission cross sections and k_{ex} has been established for this simulation by measuring the prompt jumps. Variation of the fission cross sections as a function of time is the means used to perturb the simulated system.

IV. COMPUTING TECHNIQUES

Ideally, a hybrid computer should have enough analog and digital components and enough flexibility among these so that decisions as to how to arrange the simulation of a mathematical model can be based on logic and economics. At this stage in the development of the hybrid computer, this condition rarely exists. The model is usually restricted by the capacity of the computing system, and the arrangement of the simulation is dictated by the type of computing components available in the system.

Argonne's hybrid is small, and most of its components are analog. However, all equations in this model are programmed both for a digital computer in FORTRAN IV and for an analog computer, thus providing flexibility, should the hybrid be expanded to include more digital or analog components.

The limited amount of equipment dictates that both the neutronic and thermodynamic equations be put on analog components. The present digital components are used for computing feedback, for storing information, and for setting the potentiometers of the analog components.

If the Argonne system were large enough, the best way to program this model would be to put the equations of the thermodynamic phenomena (which have long time constants) and the feedback equations (which are algebraic) on the digital components, and the highly nonlinear neutronic equations (which have relatively very short time constants) on the analog components.

The technique of simulating this specific mathematical model on Argonne's hybrid computer differs from one of the previous simulations contained in a paper by Sanathanan et al.[1] in that the two-group, space- and time-dependent diffusion equations are used instead of the one group or point kinetics.

The procedure for performing the time-dependent simulation is as follows:

1. The steady-state conditions associated with the initial power level desired are determined first.

2. The system of equations defines conditions within the volume of an axial increment of the cylindrical core. The volume of the core is covered by multiplexing this system of equations.

3. At each axial increment, the reactivity feedback resulting from a forced variation of the energy-dependent neutron cross sections is calculated and stored in the computer memory.

4. The exit coolant temperature from the first axial increment becomes the inlet temperature to the second axial increment, and so on, until the volume of the core is covered. The axial temperatures are averaged over a region, and the resulting feedback is calculated. The calculation is repeated until convergence is achieved. The volumetric increments are so tightly coupled that if the sum converges, each of its parts also converge.

The feedback used on iteration n is calculated from the temperature distribution computed in run n - 1. Initially, the feedback is set equal to zero in most cases, but for large steps it is set equal to a large enough negative value to prevent the neutron flux, during the first iteration, from becoming excessive.

Since the iteration scheme introduces a fictitious delay equal to the problem-solution time for the feedback, there arises a possibility of introducing instabilities into the simulated reactor system due entirely to the method of computation. Such was found to be the case, and a damping method was introduced.

One way of overcoming this problem of computational instability is to use a decelerating factor W, such that $0 < W < 1$.

The feedback used in iteration $(n + 1)$ = W x feedback computed from data in iteration $(n - 1) + (1 - W)$ feedback computed from data in iteration (n).

W does not affect the convergence, but does damp the functional instability as is shown in Figs. 5 and 6 where W is 0.50 and 0.85, respectively.

The iteration is initiated by making an initial guess for the feedback as a function of time. The corresponding transient neutron flux and the temperatures are determined. The digital components of the hybrid computer now calculate a new feedback concomitant with the temperatures. This feedback is then used in the next iteration. The iterative process is continued until the required convergence of the system variables is achieved.

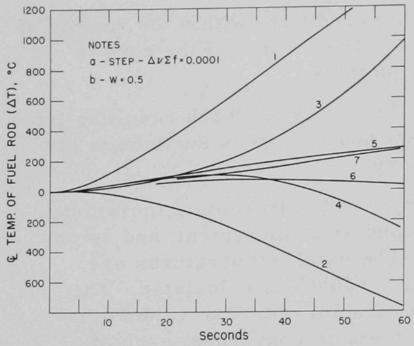

Fig. 5. Response of Model to a Step Increase of Fission Cross Section with W = 0.50. ANL Neg. No. 113-2639.

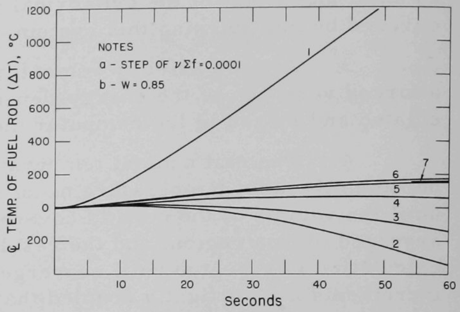

Fig. 6. Response of Model to a Step Increase of Fission Cross Section with W = 0.85. ANL Neg. No. 113-2637.

The neutron equations are very sensitive to the net amount of reactivity, especially when this amount approaches the value that makes the reactor prompt critical. Consequently, in the simulation of transients involving the addition of large amounts of reactivity, the domain of convergence becomes restricted; and if the iteration begins with a poor initial guess of the feedback, a large number of iterations usually are necessary to achieve convergence. As the neutron lifetime becomes shorter, the sensitiveness of the kinetics equations increases rapidly and the rate of convergence of the iterative process becomes slower. The success of this scheme for hybrid simulation depends to a large extent upon the rate of convergence. It therefore becomes imperative to find techniques by means of which one can guarantee convergence in a relatively small number of iterations. This is one of the objectives of this first phase of the work.

Another objective is the investigation of the effects of sampling rate. High sampling rates improve accuracy. However, the digital memory capacity becomes a limiting factor when long-duration transients have to be analyzed. Consequently, there is an optimum rate. A relatively small sampling rate is adequate to represent all the frequency contents in the temperature response. The feedback corresponding to the temperature samples is fed into the neutron-diffusion equations, which have a very high frequency response.

Most of the existing hybrid computers today have small digital memory capacity. Hence, one is very limited in terms of flexibility in storing programs and data in the active core. The iterative scheme of this report requires the facility to store large amounts of data. Also, since the improved method of simulation facilitates the computation of long-duration transients in a single stage, the need for the storage space becomes acute. The use of a disk partially circumvents this difficulty.

Long-duration transients can also be simulated in several stages. Convergence, then, is achieved in each consecutive stage.

A limited digital memory also makes the investigator search for minimum sampling rates. A good deal of research has been done to investigate the effect of sampling rates in the D/A and A/D conversions involved in hybrid computing.[1] The relative sizes of the sampling intervals have considerable effect on the accuracy of the computed response of the closed-loop reactor system, whose categories of phenomena have widely varying frequency-response characteristics. However, at present, there appears to be no relatively easy way of analytically determining the minimum adequate sampling rates.

The system shown in Fig. 2 is in a steady state. The inlet conditions to each radial increment on the plane Z_0 are given. An arbitrary change in any time-dependent variable in any category can be made. The variable in this simulation is the fission cross sections in core region 1.

The convergence may be illustrated by plotting a number of system variables against time. In this case, the temperature of the fuel in region one is used, and the rate and number of iterations are shown on Figs. 5-8. The forcing function is the fission cross section in the form of jumps, ramps, and sine waves.

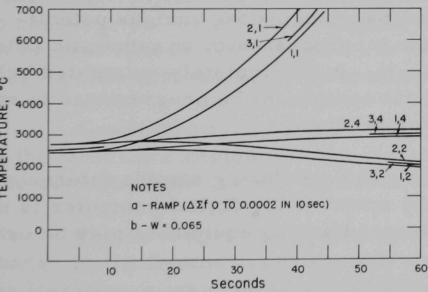

Fig. 7. Response of the Model to a Ramp Increase of Fission Cross Section with W = 0.65. ANL Neg. No. 113-2636.

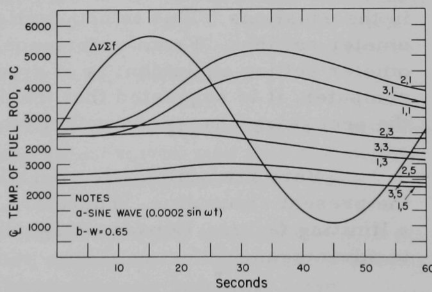

Fig. 8. Response of the Model to a Sine Wave in Fission Cross Section. ANL Neg. No. 113-2638 Rev. 1.

V. GENERAL DISCUSSION

The outstanding feature of the present method of analyzing the response of a closed-loop system is the iterative procedure and the sampling rate. This allows multiplexing of computer components.

As a result of multiplexing, there is a large saving in analog circuitry. But for this economy of computer facilities, it would not have been possible to handle the number of differential equations in even this simple mathematical model of the reactor core.

The success of the present method of analyzing the response of any closed-loop system depends essentially upon the convergence of the iterative process. From a practical standpoint, a mathematical proof of convergence alone is not enough. Simulation of typical transients is necessary to obtain a quantitative estimate of the necessary number of iterations.

The iterative process has facilitated simulation in continuous time for rather large intervals of time. The length of the time interval is limited only by practical considerations, such as the available memory, required sampling rate, and necessary number of iterations for convergence. If the response needs to be computed for a long interval, this interval may be subdivided into smaller intervals (whose length is compatible with the practical limitations) and the response computed sequentially. When convergence depends upon the response time, a large saving in computing time and memory units is possible by subdividing the response time.

One practical aspect of multiplexing of analog circuitry is the frequent reinitialization of the variables and the modification of the parameters in the equations. This is accomplished by changing the various potentiometer settings. From experience, the incorporation of an automatic potentiometer setting equipment is of great help. In a completely automated hybrid computer, it is suggested that the digital component be programmed to effect the necessary changes in potentiometer settings.

Very few arithmetic operations are done during sample intervals in the present simulation. Therefore, the speed of the digital computer is not a limiting factor. Consequently, high-speed analog equipment may be used to advantage.

The hybrid simulation is proving itself to be effective and economical in the analysis of transience in normal nuclear-reactor operations and in hypothetical accident conditions. This simulation can be particularly useful in the design studies of fast-reactor cores composed of ceramic fuels whose thermal properties vary significantly with temperature.

The techniques used in the hybrid simulation are general enough to be applicable to many dynamic systems with feedback. The advantages of the techniques increase with the amount of multiplexing and the degree of complexity in the equations. It is therefore recommended that further effort be made to demonstrate the applicability of this method of simulation to other mathematical models composed of nonlinear partial differential equations.

VI. RESULTS

The simulation of the model upon the computer gives, as a function of time, the fuel and coolant temperatures and the neutron flux in each volume increment of the reactor core. When any variable, such as a cross section or a physical property of core material, is perturbed, the computer will try to restore the model to the equilibrium of all interacting phenomena. This usually results in a change in power level and temperature throughout the core. Anything that happens to any variable in the equation comprising the model affects to some extent all other energy-, space-, and time-dependent variables in the system. For example, a change in the reflector material cross sections affects the neutron balance in every region of the core and in turn affects the power level.

All the variables in the model can be displayed as a function of time.

Since it was necessary to cover the volume of the core by multiplexing the equations common to equidistant bounded planes concentric with and perpendicular to the longitudinal axis of the core, it was necessary to converge on some time-dependent variable in the set of equations such as neutron flux or temperature. In this case, the average temperature of fuel was the variable upon which convergence was achieved.

A perturbation of the fission cross section in the neutronic equations of the first core region was the disturbing effect introduced into the system. The perturbations were in the form of a step, a ramp, and a sine wave.

Figure 5 shows the convergence characteristics in response to a step change in the fission cross section of core region No. 1. Since the feedback for iteration n was computed from the temperatures resulting from iteration n - 1, there is some instability due to overcorrection resulting from the time span of the calculation.

Figure 6 shows how an increase in the value of W from 0.50 in Fig. 5 to 0.85 reduces the instability and also reduces the number of iterations required to achieve convergence.

Figure 7 shows how the system converges after a ramp change in the fission cross sections of region 1.

Figure 8 shows how the system converges after the initiation of a sinusoidal variation in the value of the fission cross sections of region one.

Rather long run times were chosen, since one purpose of the calculation was a desire to see if a kinetics model that was capable of giving good short-time dynamic accuracy could also be made stable over rather long time intervals.

VII. CONCLUSIONS

Currently the hybrid computers are beginning to show potentialities for the simulation of nuclear-reactor transients. This is due to the following features, characteristic of any hybrid system:

1. The ease and efficiency of simulating a large set of nonlinear differential equations of the model.

2. A low probability of numerical instabilities, which are frequently a source of anxiety in the pure digital simulation of coupled partial differential equations.

3. Simplicity of programming.

4. Economy resulting from a substantial reduction of the expensive hardware; and programming effort.

APPENDIX A

Nuclear and Heat-transfer Data

1. Nuclear Data

a. Two-group Constants

Group 1--Energy 1.35 MeV to ∞

$\chi_1 = 0.575$

Isotope	ν	σ_f	σ_s	σ_{tr}	σ_{1s2}
^{239}Pu	3.10	1.95	0.10	4.6	0.90
^{235}U	2.7	1.29	0.08	4.5	1.50
^{238}U	2.6	0.524	0.036	4.6	2.05
Fe	-	-	0.005	2.0	0.70
Na	-	-	0.0005	2.0	0.30
Al	-	-	0.004	1.8	0.38

Group 2--Energy 0 to 1.35 MeV

$\chi_2 = 0.425$

Isotope	ν	σ_f	σ_s	σ_{tr}	σ_{1s2}
^{239}Pu	2.93	1.78	0.30	7.0	-
^{235}U	2.5	1.44	0.28	7.2	-
^{238}U	2.47	0.005	0.19	7.1	-
Fe	-	-	0.006	2.8	-
Na	-	-	0.0008	3.5	-
Al	-	-	0.002	3.5	-

b. Macroscopic Cross Sections

(1) Core Region--Group 1

Isotope	% Vol	atoms/cc x 10^{-24}	Σ_a	Σ_f	Σ_s	Σ_{tr}
^{235}U	15.07	0.0473	0.0149	0.0092	0.0107	0.0321
^{238}U	1.13	0.0473	0.0003	0.0003	0.0011	0.0025
O	16.20	0.0919	0	0	0.0566	0.0499
Na	54.87	0.0254	0	0	0.0042	0.0279
SS	12.73	0.0847			0.0075	0.0216
			0.0152	0.0095	0.0801	0.1340

$D_{i,i} = 0.2488$

(2) Core Region--Group 2

Isotope	% Vol	atoms/cc x 10^{-24}	Σ_a	Σ_f	Σ_s	Σ_{tr}
^{235}U	15.07	0.0473	0.0123	0.0103		0.0513
^{238}U	1.13	0.0473	0.0001			0.0038
O	16.20	0.0919				0.0499
Na	54.87	0.0254				0.0488
SS	12.73	0.0847				0.0302
			0.0124	0.0103	0	0.1840

$D_{2,i} = 1.81$

(3) Reflector--Group 1

			Σ_a	Σ_f	Σ_s	Σ_{tr}
Be	70.00	0.01229			0.4646	0.4302
Na	20.00	0.0254			0.0015	0.0102
SS	10.00	0.0847			0.0059	0.0169
			0	0	0.4720	0.4573

$D_{1,i} = 0.7289$

(4) Reflector--Group 2

			Σ_s	Σ_{tr}
Be	70.00	0.01229	0.4646	0.4302
Na	20.00	0.0254	0.0015	0.0102
SS	10.00	0.0847	0.0059	0.0169
			0.4720	0.4573

$D_{2,i} = 0.7289$

c. Delayed Neutron

Group	λ_i	t_i	β_i	$\beta_i t_i$	C_i
1	1.3×10^{-2}	76.9231	7.62×10^{-5}	5.861×10^{-3}	1.24×10^{4}
2	3.14×10^{-2}	31.8471	6.27×10^{-4}	1.997×10^{-2}	4.22×10^{4}
3	1.36×10^{-1}	7.3529	5.61×10^{-4}	4.125×10^{-2}	8.72×10^{4}
4	3.4×10^{-1}	2.9412	1.06×10^{-3}	3.118×10^{-3}	0.659×10^{4}
5	1.32	0.7576	4.8×10^{-4}	3.636×10^{-4}	0.076×10^{4}
6	3.5	0.2857	3.5×10^{-4}	1.000×10^{-4}	0.021×10^{4}

$\ell = 4.728 \times 10^{-7}$ $\Sigma\beta_i = 0.003154$

When the six groups of delayed neutrons are reduced to one group, $C_1 = 70,900$.

2. Heat-transfer Data

Specific heat of sodium	C_p =	1.26	W-sec/g °K
Density of sodium	ρ =	0.9712	g/cm^3
Specific heat x density of UO_2	$C_p \times \rho$ =	3.45	J/cm^3 x °K
Density of UO_2	ρ =	10.8	g/cm^3
Specific heat of UO_2	C_p =	0.32	W-sec/g °K
Thermal conductivity UO_2	K =	0.03	W/cm °K
Temperature of sodium	T =	500°K (inlet)	°K
Heat-transfer coefficient	H =	5.67	W/cm °K
Radial increment	W =	0.060	cm
Mass flow of sodium	G =	400	g/cm^2-sec
Axial increment	Δz =	1.5	cm
$\frac{\text{Circumference of rod}}{\text{Flow area}}$	Λ =	1.0	cm^2/cm^3
Velocity of coolant	V =	635.77	cm/sec
Length of rod	L =	150.0	cm
Diameter of rod	D_r =	0.548	cm
Diameter of cladding	D_c =	0.635	cm
Cladding thickness	h =	0.039	cm

APPENDIX B

Computing Programs

1. Analog Program

a. Neutron-diffusion Equations

The neutron-diffusion equations (Eqs. 1-3) are transformed for the analog as follows. The analog diagram of these equations is shown in Fig. 9.

(1) Core Region 1--Group 1

Region radii = 0 to 40 cm Region length = 150 cm

$$\frac{d\Phi_{1,1}}{dt} = -\frac{\mathscr{D}_{1,1}S_{0,2}v_{1,1}}{V_{0,1}}(\Phi_{1,1}-\Phi_{1,2}) - (\Sigma_{1,1,a}+\Sigma_{1,1,s}+D_{1,1}B_z^2)(v_{1,1}\Phi_{1,1})$$

$$+ (X_{1,0}v_{1,0})(\nu_{1,1}\Sigma_{1,1,f_0}\Phi_{1,1}+\nu_{2,1}\Sigma_{2,1,f_0}\Phi_{2,1})$$

$$- (\beta X_{1,0}v_{1,1})(\nu_{1,1}\Sigma_{1,1,f_0}\Phi_{1,1}+\nu_{2,1}\Sigma_{2,1,f_0}\Phi_{2,1}) + (X_{1,0}v_{1,1})(\lambda_{1,1}C_1)$$

$$+ (X_{1,0}v_{1,1})(\Delta\nu_{1,1}\Sigma_{1,1,f}\Phi_{1,1}+\Delta\nu_{2,1}\Sigma_{2,1,f}\Phi_{2,1}). \qquad (B.1)$$

(2) Core Region 1--Group 2

$$\frac{d\Phi_{2,1}}{dt} = -\frac{\mathscr{D}_{2,1}S_{0,1}v_{2,1}}{V_{0,1}}(\Phi_{2,1}-\Phi_{2,2}) - (\Sigma_{2,1,a}+\Sigma_{2,1,s}+D_{2,1}B_2^2)\,v_{2,1}\Phi_{2,1}$$

$$+ \Sigma_{1,1,s}v_{1,1}\Phi_{1,1} + (X_{2,0}v_{2,1})(\nu_{1,1}\Sigma_{1,1,f_0}\Phi_{1,1}+\nu_{2,1}\Sigma_{2,1,f_0}\Phi_{2,1})$$

$$- (\beta X_{2,0}v_{2,1})(\nu_{1,1}\Sigma_{1,1,f_0}\Phi_{1,1}+\nu_{2,1}\Sigma_{2,1,f_0}\Phi_{2,1}) + (X_{2,0}v_{2,1})(\lambda_1 C_1)$$

$$+ (X_{2,0}v_{2,1})(\Delta\nu_{1,1}\Sigma_{1,1,f}\Phi_{1,1}+\Delta\nu_{2,1}\Sigma_{2,1,f}\Phi_{2,1}). \qquad (B.2)$$

(3) Core Region 1--Delayed Neutrons

$$\frac{dC_1}{dt} = \nu_{1,1}\Sigma_{1,1,f}\beta\Phi_{1,1} + \nu_{2,1}\Sigma_{2,1,f}\beta\Phi_{2,1} - \lambda C_1. \qquad (B.3)$$

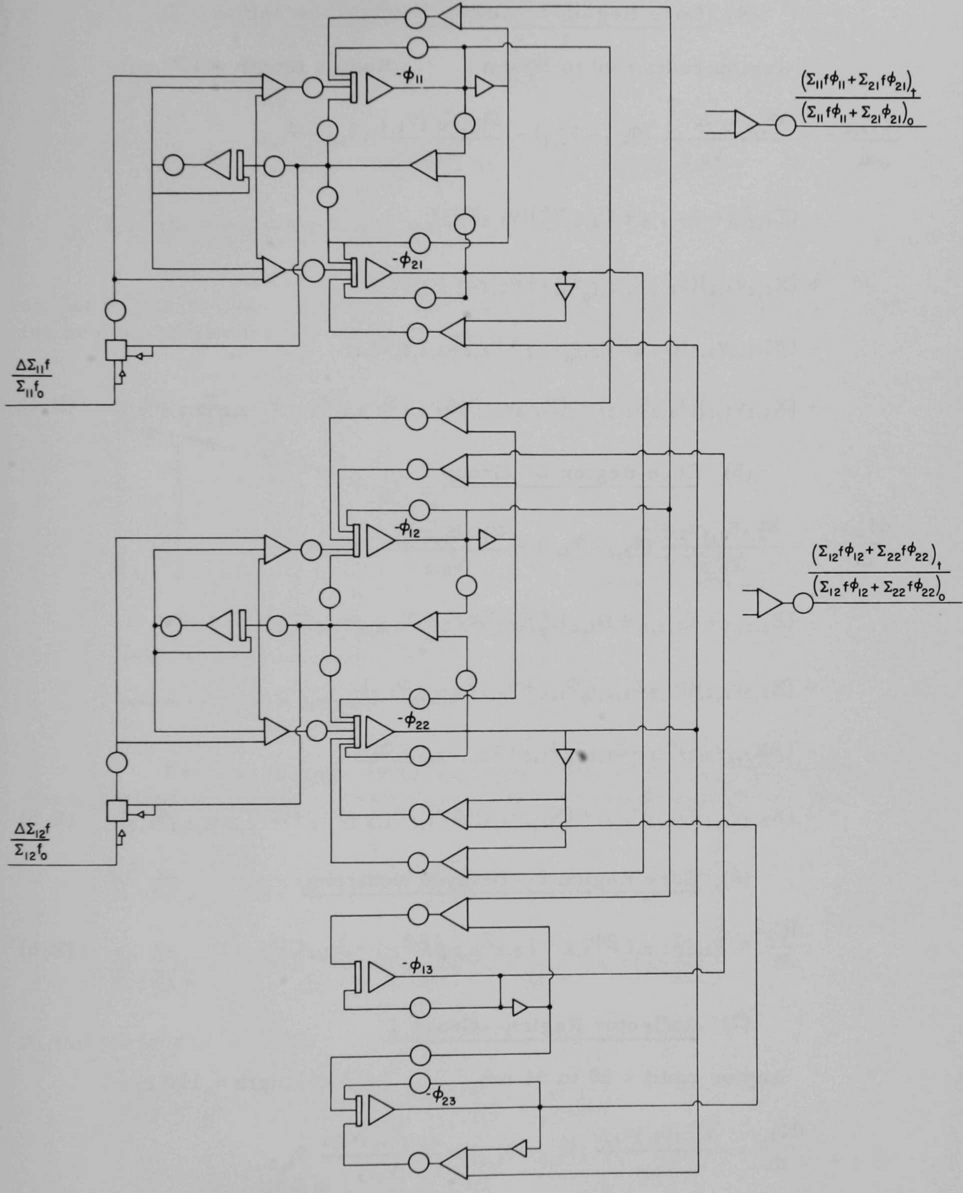

Fig. 9. Analog Diagram of the Diffusion Equations

(4) Core Region 2--Group 1

Region radii = 40 to 50 cm   Region length = 150 cm

$$\frac{d\Phi_{1,2}}{dt} = -\frac{\mathcal{D}_{1,1}S_{0,2}v_{1,2}}{V_{0,2}}(\Phi_{1,2}-\Phi_{1,1}) - \frac{\mathcal{D}_{1,2}S_{0,2}v_{1,2}}{V_{1,2}}(\Phi_{1,2}-\Phi_{1,3})$$

$$-(\Sigma_{1,2,a}+\Sigma_{1,2,s}+D_{1,2}B_z^2)(v_{1,2}\Phi_{1,2})$$

$$+(X_{1,2}v_{1,2})(\nu_{1,2}\Sigma_{1,2,f_0}\Phi_{1,2}+\nu_{2,2}\Sigma_{2,2,f_0}\Phi_{2,2})$$

$$-(\beta X_{1,2}v_{1,2})(\nu_{1,2}\Sigma_{1,2,f_0}\Phi_{1,2}+\nu_{2,2}\Sigma_{2,2,f_0}\Phi_{2,2})$$

$$+(X_{1,2}v_{1,2})(\lambda_{1,2}C_{1,2})+(X_{1,2}v_{1,2})(\Delta\nu_{1,2}\Sigma_{1,2,f_0}\Phi_{1,2}+\nu_{2,2}\Sigma_{2,2,f}\Phi_{2,2}). \quad \text{(B.4)}$$

(5) Core Region 2--Group 2

$$\frac{d\Phi_{2,2}}{dt} = -\frac{\mathcal{D}_{2,1}S_{0,1}v_{2,2}}{V_{0,2}}(\Phi_{2,2}-\Phi_{2,1}) - \frac{\mathcal{D}_{2,2}S_{0,3}v_{2,2}}{V_{0,2}}(\Phi_{2,2}-\Phi_{2,3})$$

$$-(\Sigma_{2,2,a}+\Sigma_{2,2,s}+D_{2,2}B_z^2)(v_{2,2}\Phi_{2,2}+\Sigma_{1,2,s}v_{2,2}\Phi_{1,2})$$

$$+(X_{2,2}v_{2,2})(\nu_{1,2}\Sigma_{1,2,f_0}\Phi_{1,2}+\nu_{2,2}\Sigma_{2,2,f_0}\Phi_{2,2})$$

$$-(\beta X_{2,2}v_{2,2})(\nu_{1,2}\Sigma_{1,2,f_0}\Phi_{1,2}+\nu_{2,2}\Sigma_{2,2,f_0}\Phi_{2,2})$$

$$+(X_{2,2}v_{2,2})(\lambda_{2,2}C_{2,2})+(X_{2,2}v_{2,2})(\Delta\nu_{1,2}\Sigma_{1,2,f}\Phi_{1,2}+\Delta\nu_{2,2}\Sigma_{2,2,f}\Phi_{2,2}). \quad \text{(B.5)}$$

(6) Core Region 2--Delayed Neutrons

$$\frac{dC_2}{dt} = \nu_{1,2}\Sigma_{1,2,f}\,\beta\Phi_{1,2}+\nu_{2,2}\Sigma_{2,2,f}\,\beta\Phi_{2,1}-\lambda_{2,2}C_2. \quad \text{(B.6)}$$

(7) Reflector Region--Group 1

Region radii = 50 to 56 cm   Region length = 150 cm

$$\frac{d\Phi_{1,3}}{dt} = -\frac{\mathcal{D}_{1,2}S_{0,3}v_{1,3}}{V_{0,3}}(\Phi_{1,3}-\Phi_{1,2}) - \frac{J_{1,3}S_{0,4}v_{1,3}}{V_{0,3}}\Phi_{1,3}$$

$$-(\Sigma_{1,3,a}+\Sigma_{1,3,s}+D_{1,3}B_z^2)\,v_{1,3}\Phi_{1,3}. \quad \text{(B.7)}$$

(8) Reflector Region--Group 2

$$\frac{d\Phi_{2,2}}{dt} = -\frac{\mathscr{D}_{2,2}S_{0,3}v_{2,3}}{V_{0,3}}(\Phi_{2,3} - \Phi_{2,2}) - \frac{J_{2,3}S_{0,4}v_{2,3}\Phi_{2,3}}{V_{0,3}}$$

$$- (\Sigma_{2,3,2} + \Sigma_{2,3,s} + D_{2,3}B_z^2)\, v_{2,3}\Phi_{2,3} + \Sigma_{1,3,s}v_{2,3}\Phi_{1,3}\,. \qquad \text{(B.8)}$$

b. Heat-transfer Equations

The equations for each Δz of the three fuel rods are identical except for the initial conditions. The increments of the radius of a fuel rod for analog computation is shown in Fig. 10.

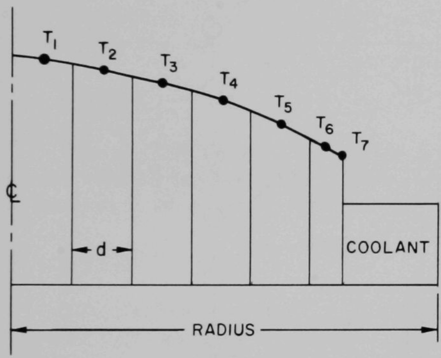

Fig. 10

Radial Temperature Profile in a Fuel Rod

The analog diagram for an axial segment Δz is given on Fig. 11. The equations in a form suitable for analog components are as follows:

$$\left.\begin{aligned} \frac{C\rho}{K}\frac{\partial T}{\partial t} &= \left[\frac{1}{r}\frac{\partial T}{\partial r} + \frac{\partial^2 T}{\partial r^2}\right] + \frac{q}{K}(r,z,t); \\ \frac{C\rho}{K}\frac{\partial T}{\partial t} &= \frac{1}{r}\left(\frac{T_{i+1} - T_{i+1}}{2h}\right) + \left(\frac{T_{i+1} - 2T_i + T_{i-1}}{h^2}\right) + \frac{q}{K}. \end{aligned}\right\} \qquad \text{(B.9)}$$

At the surface of the rod,

$$\left.\begin{aligned} -\frac{\partial T}{\partial r} = \frac{H}{K}(T_s - \overline{T}_c), \quad \frac{T_7 - T_6}{h/2} &= \frac{H}{K}(T_7 - \overline{T}_c), \\ T_7 = \left(T_6 - \frac{H}{K}\frac{h}{2}\overline{T}_c\right) &\Big/ \left(1 - \frac{H}{K} \times \frac{h}{2}\right). \end{aligned}\right\} \qquad \text{(B.10)}$$

$$\left.\begin{aligned} &\frac{\partial}{\partial t}(C\rho\,\overline{T}_c) + \frac{\partial}{\partial z}(G\cdot C,\ \overline{T}_c) = \Lambda Q; \\ &\overline{T}_{cj} = \frac{T_{cj1} + T_{cj2}}{2}. \end{aligned}\right\} \qquad (B.11)$$

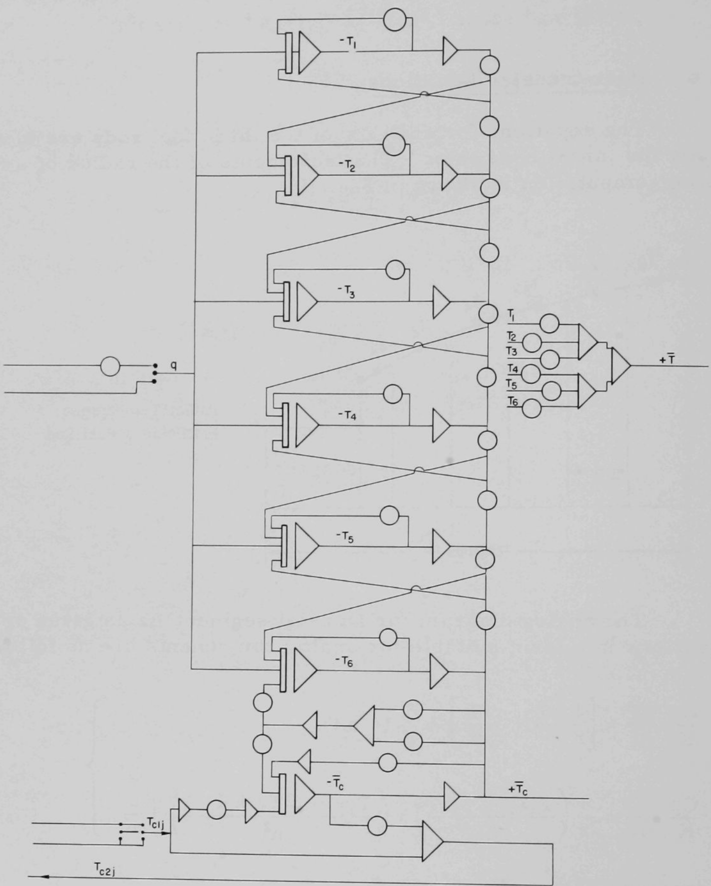

Fig. 11. Analog Diagram of the Heat-transfer Equations

2. Digital Computing Program

a. The Digital Program

The computer part of the hybrid was an IBM 1130 with 8K of core storage and a disk storage with a capacity of about 350K after allowance for the storage of the IBM system and the subroutine library. This system dictated, to a large extent, the following division of the digital code into three mainline programs and one subroutine. The program modules are described below.

b. CRTR1

The CRTR1 module provides for entering on the console typewriter the total number of A to D samples per solution, the number of milliseconds between samples, and the number of axial sections.

Provision is also made for reading from cards into a 20 x 20 array the initial temperatures for each axial section.

The initial reactivities and inlet are also read and stored on the disk ready for the first run.

c. CRTR2

The CRTR2 module is executed over for each run. Potentiometers are set for the initial temperature distribution of each axial section. The A/D converter is readied, and the analog is started.

d. CRTRF

The CRTRF is the ISS subroutine associated with the A/D converter. Every time an A/D complete interrupt is received by the 1130, this subroutine is executed. The data are stored in blocks of 10 words in a 10 x 64-word buffer. Half of the buffer is stored on the disk 1 by CRTR2 at the same time that the other half is being filled with data by CRTRF. When the iteration is done, CRTR3 is then executed.

e. CRTR3

This module computes the new reactivities from the average temperatures. The new reactivities are then loaded into the disk memory together with the inlet temperatures for axial region 1, and a new iteration is begun by executing CRTR2 again.

The flow chart for the IBM 1130 is shown on Fig. 12.

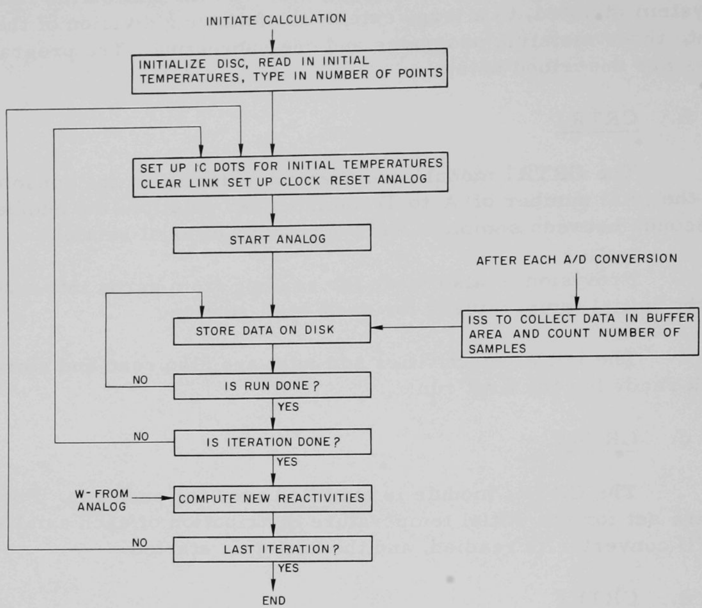

Fig. 12. Digital-computer Flow Chart

REFERENCE

1. C. K. Sanathanan, J. C. Carter, L. T. Bryant, and L. W. Amiot, "Hybrid Computers In The Analysis of Feedback Control System," *Proceedings of the Fall Joint Computer Conference, November 7-10, 1966*, San Francisco, California.